

Article

Synthesis, Crystal Structure, and Antifungal Activity of Quinazolinone Derivatives

Rong Zeng¹, Cong Huang¹, Jie Wang², Yuan Zhong¹, Qingwen Fang¹, Shuzhen Xiao², Xuliang Nie², Shangxing Chen^{1,*}  and Dayong Peng^{2,*} 

¹ East China Woody Fragrance and Flavor Engineering Research Center of National Forestry and Grassland Administration, College of Forestry, Jiangxi Agricultural University, Nanchang 330045, China; 15070876102@163.com (R.Z.); huangc5020@163.com (C.H.); zhongy9897@163.com (Y.Z.); fqw912029833@126.com (Q.F.)

² Key Laboratory of Chemical Utilization of Plant Resources of Nanchang, East China Woody Fragrance and Flavor Engineering Research Center of National Forestry and Grassland Administration, College of Chemistry and Materials, Jiangxi Agricultural University, Nanchang 330045, China; wangjie951127@163.com (J.W.); xiao888612@163.com (S.X.); 13576953044@163.com (X.N.)

* Correspondence: csxing@126.com (S.C.); dayongpeng@163.com (D.P.)

Abstract: In this paper, four new compounds with quinazolinone structure were designed and synthesized based on the special biological activity of quinazolinone. The four new compounds containing quinazolinone structures were synthesized using a one-pot method after intramolecular cyclization and dehydration catalyzed by aqueous methylamine solution. Their structures were characterized using ¹H NMR, ¹³C NMR, FT-IR, and HRMS, and the crystal structure of **2a** was characterized using X-ray diffraction. In their potential antifungal activity tests, it was found that the four newly synthesized compounds exhibited significant antifungal activity against all seven phytopathogenic fungi at concentrations of 150 and 300 mg/L. Among them, the target compound **2c** showed the best inhibitory effect against *Fusarium oxysporum* f. sp. *Niveum* fungus, with 62.42% inhibition at a concentration of 300 mg/L. Compound **2c** is expected to be a leading compound for the treatment of watermelon *Fusarium wilt* in the future, which is worth further study.

Keywords: quinazolinone; synthesis; antifungal activity



Citation: Zeng, R.; Huang, C.; Wang, J.; Zhong, Y.; Fang, Q.; Xiao, S.; Nie, X.; Chen, S.; Peng, D. Synthesis, Crystal Structure, and Antifungal Activity of Quinazolinone Derivatives. *Crystals* **2023**, *13*, 1254. <https://doi.org/10.3390/cryst13081254>

Academic Editor: Duane Choquesillo-Lazarte

Received: 31 July 2023

Revised: 7 August 2023

Accepted: 11 August 2023

Published: 14 August 2023



Copyright: © 2023 by the authors. Licensee MDPI, Basel, Switzerland. This article is an open access article distributed under the terms and conditions of the Creative Commons Attribution (CC BY) license (<https://creativecommons.org/licenses/by/4.0/>).

1. Introduction

Plant diseases cause 10–15% loss of the world's main crops every year, and direct economic losses reach hundreds of billions of dollars [1]. Among them, 70–80% of plant diseases are caused by pathogenic fungi [2]. Over the years, plant phytopathogenic fungi have caused extremely serious losses to crop cultivation around the world, drastically affecting crop yield and quality, and have also becoming an important bottleneck for sustainable agricultural development [3]. The application of chemical pesticides in agricultural production is one of the most effective ways to prevent damage to agricultural crops from phytopathogenic fungi. In the last decade, the global sales of agricultural fungicides have been increasing year by year. The prevention and control of plant phytopathogenic fungi has also become a hot topic in modern pesticide chemistry research.

Many N-heterocyclic compounds are widely distributed in nature and have high physiological and pharmacological activities. The main reason is that the presence of N atoms changes the electronic arrangement of the ring, which directly affects the physical and chemical properties of N-containing heterocycles [3]. They are components of many important biomolecules, including many vitamins, nucleic acids, drugs, antibiotics, and pesticides [4]. Among them, nitrogen-containing compounds also widely exist in the field of pesticide chemistry, and nitrogen-containing groups are often the core reason for their biological activities [5]. Quinazolinones compounds are a unique group of aromatic

compounds with a benzo-fused heterocyclic structure, which have attracted much attention due to their broad and unique biological activities [6]. Due to the double-ring structure of benzene ring and pyrimidine ring, it increases the possibility and flexibility of structural modification [7] and shows great potential in the discovery of new pesticides [8]. In the field of pesticides and medicine, researchers have identified many biological activities of quinazolinone derivatives, including antifungal, insecticidal, antiviral, anti-cytotoxic, antispasmodic, antitubercular, antioxidant, antimalarial, antihypertensive, etc., and hence, they have been widely used [9–15]. Pyrazole and pyridine are typical representatives of simple azo-containing heterocyclic groups. Many compounds with high biological activity are widely used to develop new and efficient pesticides such as fungicides, herbicides, and pesticides because of the existence of such groups [16]. The connection between pyrazole and quinazolinone is expected to combine their excellent biological activities. Habib, O. M. et al. [17] demonstrated that pyrazol-quinazolinone has good antifungal and antibacterial effects. The potential biological activity of quinazolinone prompted us to search for compounds with similar structures.

In this study, four novel pyrazol-quinazolinone compounds with different substituents were synthesized. The target compounds contain quinazolinone, pyrazole, pyridine, and other high-activity groups, in order to combine them to obtain new compounds with higher biological activity. Their structures were characterized using ^1H NMR, ^{13}C NMR, FT-IR, HRMS, and X-ray diffraction, and their antifungal activity was studied, in order to find new structural clues and provide basis for their use as effective antifungal agents. This study may provide theoretical support for the research of quinazolinone antifungal drugs, and it is of great significance to fill the gap in the current market of such antifungal agents.

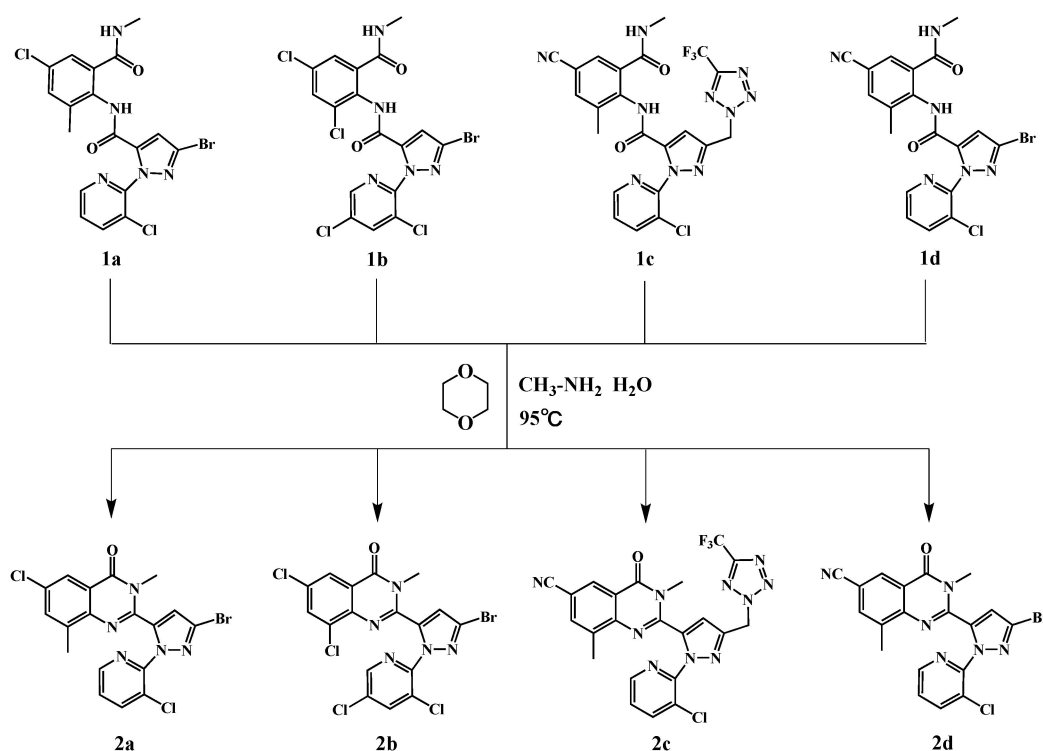
2. Experimental

2.1. Materials and Methods

All chemicals were commercially purchased and were of reagent grade and did not need purification. All plant fungi were provided by the Plant Pathology Laboratory of Agricultural College of Jiangxi Agricultural University. FT-IR spectra of the samples were performed between 400 and 4000 cm^{-1} using KBr pellets. ^1H NMR and ^{13}C NMR spectra were performed using AV 400 MHz spectrometer (CDCl_3 as solvents). High-resolution mass spectrometry (HRMS) spectra were recorded on a triple time-of-flight TOF 5600+ (AB Sciex) mass spectrometer (Concord, ON, Canada). The melting point of the compound was measured with a melting point instrument (44X-6T). The X-ray analysis of the samples was recorded on a Bruker APEX II area detector diffractometer at 296(2) K with graphite-monochromatic $\text{MoK}\alpha$ radiation ($\lambda = 0.71073 \text{ \AA}$).

2.2. Syntheses of Compounds 2a~2d

The reaction substances (compound **1a**, 10 g, 20 mmol), 1,4-dioxane (40 mL), and approximately 1% of methylamine aqueous solution were sequentially added to a round-bottom flask equipped with a stirrer, with full stirring, and 400 mL of distilled water was added, and the reaction was carried out at 90 °C for 4 h. The reaction was monitored using TLC (petroleum ether/ethyl acetate = 2:1, *v/v*). The resulting precipitate was filtered under vacuum, washed with water, and dried in air. The crude product was purified using column chromatography (silica gel, petroleum ether/ethyl acetate = 5:1, *v/v*), and the product **2a** was obtained. Products **2b~2d** were produced with the same procedure using starting materials **1b~1d**. The synthesis path is shown in Scheme 1.



Scheme 1. Synthesis of compounds 2a~2d.

Compound 2a: White solid, yield 87.33%, m.p. 211.6~212.3 °C. FT-IR ν (cm^{-1}): 3127, 2073, 2956, 1670, 1587, 1523, 1465, 794. ^1H NMR (400 MHz, CDCl_3) δ 8.36 (dd, $J = 1.60, 4.65$ Hz, 1H), 8.09 (d, $J = 2.59$ Hz, 1H), 7.86 (dd, $J = 1.60, 8.01$ Hz, 1H), 7.43 (d, $J = 1.53$ Hz, 1H, pyr-H), 7.33 (dd, $J = 4.73, 7.93$ Hz, 1H), 6.86 (s, 1H), 3.79 (s, 3H, N-CH₃), 2.03 (s, 3H, ph-CH₃). ^{13}C NMR (100 MHz, CDCl_3) δ 161.4, 148.4, 146.9, 144.2, 143.6, 139.5, 138.6, 138.4, 135.0, 133.2, 128.2, 127.9, 125.1, 123.7, 121.5, 111.9, 33.6, 16.5. HRMS calculated for $\text{C}_{18}\text{H}_{12}\text{BrCl}_2\text{N}_5\text{O}$ $[\text{M}+\text{H}]^+$ 463.9681, found 463.9661.

Compound 2b: White solid, yield 84.52%, m.p. 183.2~183.7 °C. FT-IR ν (cm^{-1}): 3126, 3080, 3049, 2967, 1681, 1593, 1525, 1463, 793. ^1H NMR (400 MHz, CDCl_3) δ 8.26 (d, $J = 2.29$ Hz, 1H), 8.15 (d, $J = 2.44$ Hz, 1H), 7.88 (d, $J = 2.29$ Hz, 1H, pyr-H), 7.69 (d, $J = 2.44$ Hz, 1H), 6.87 (s, 1H), 3.77 (s, 3H, N-CH₃). ^{13}C NMR (101 MHz, CDCl_3) δ 160.6, 146.6, 145.6 (d, $J = 6.97$ Hz), 141.8, 139.0, 137.9, 134.9, 133.5, 133.1, 132.7, 128.5, 128.4, 125.1, 122.5, 112.6, 33.9. HRMS calculated for $\text{C}_{17}\text{H}_8\text{BrCl}_4\text{N}_5\text{O}$ $[\text{M}+\text{H}]^+$ 519.8715, found 519.8705.

Compound 2c: White solid, yield 84.60%, m.p. 185.7~186.4 °C. FT-IR ν (cm^{-1}): 3104, 3062, 2997, 2958, 2232, 1681, 1590, 1434, 800. ^1H NMR (400 MHz, CDCl_3) δ 8.42 (d, $J = 2.29$ Hz, 1H), 8.36 (dd, $J = 1.60, 4.65$ Hz, 1H), 7.88 (dd, $J = 1.68, 8.09$ Hz, 1H, pyr-H), 7.63 (s, 1H), 7.35 (dd, $J = 4.65, 8.01$ Hz, 1H), 6.97 (s, 1H), 6.10 (s, 2H), 3.76 (s, 3H, N-CH₃), 2.02 (s, 3H, ph-CH₃). ^{13}C NMR (101 MHz, CDCl_3) δ 161.0, 148.5, 147.5, 147.1, 147.0, 145.0, 139.70, 138.2, 137.9, 136.3, 129.9, 127.8, 125.3, 120.7, 118.0, 110.7, 109.4, 51.2, 33.8, 16.5. HRMS calculated for $\text{C}_{22}\text{H}_{14}\text{ClF}_3\text{N}_{10}\text{O}$ $[\text{M}+\text{H}]^+$ 527.1071, found 527.1060.

Compound 2d: White solid, yield 81.92%, m.p. 217.4~218.2 °C. FT-IR ν (cm^{-1}): 3188, 3079, 3060, 2958, 2227, 1675, 1582, 1516, 1466, 809. ^1H NMR (400 MHz, CDCl_3) δ 8.42 (d, $J = 2.14$ Hz, 1H), 8.33 (dd, $J = 1.68, 4.58$ Hz, 1H), 7.87 (dd, $J = 1.60, 8.01$ Hz, 1H, pyr-H), 7.63 (d, $J = 1.07$ Hz, 1H), 7.32 (dd, $J = 4.65, 8.01$ Hz, 1H), 6.87 (s, 1H), 3.78 (s, 3H, N-CH₃), 2.04 (s, 3H, ph-CH₃). ^{13}C NMR (101 MHz, CDCl_3) δ 161.03, 148.28, 147.56, 146.89, 146.80, 139.66, 138.2, 138.0, 136.3, 129.8, 128.3, 127.9, 125.2, 120.8, 118.0, 112.4, 110.7, 33.8, 16.5. HRMS calculated for $\text{C}_{19}\text{H}_{12}\text{BrClN}_6\text{O}$ $[\text{M}+\text{H}]^+$ 455.0023, found 455.0010.

2.3. Structure Determination

Compound **2a** was dissolved in a mixed solution of ethanol and dichloromethane and placed at 20 °C until the solvent slowly evaporated to obtain crystals of **2a**. The crystal structure of compound **2a** was determined using single crystal X-ray diffraction. Data were acquired using a Bruker APEX II area detector diffractometer equipped with graphite monochromatic Mo K α radiation ($\lambda = 0.71073$ Å) in 2 θ scan mode, and all data were empirically corrected for adsorption with SADABS. The structures were solved using direct methods and refined using full matrix least squares on F² using SHELXTL 97 software. All non-hydrogen atoms were located using direct methods and subsequent difference Fourier syntheses. The structure of compound **2a** was refined by geometric calculations to determine the positions and thermal parameters of the hydrogen atoms bound to carbon. Crystallographic data and pertinent information are given in Table 1; selected bond lengths and selected bond angles are provided in Table 2.

Table 1. Crystallographic information of structure of **2a**.

Empirical Formula	C ₁₈ H ₁₂ BrCl ₂ N ₅ O	V (Å ³)	1860.6(5)
Formula weight (g mol ⁻¹)	465.14	Z	4
Temperature (K)	296	Dc (g cm ⁻³)	1.661
Wavelength (Å)	0.71073	μ (mm ⁻¹)	2.516
Crystal system (mm)	Monoclinic	F (000)	928
Space group	P 21/c	Crystal size (mm)	0.220 × 0.170 × 0.140
a (Å)	11.3279(18)	Θ range for data collection (°)	2.257–25.497
b (Å)	15.934(3)	Reflections collected	13,140
c (Å)	10.6668(17)	Independent reflections	3468 [R (int) = 0.0328]
α (°)	90	Goodness-of-fit on F ² (S)	1.115
β (°)	104.910(2)	Final R indices [I > 2 σ (I)]	R ₁ = 0.0324, wR ₂ = 0.0860
γ (°)	90	R indices (all data)	R ₁ = 0.0425, wR ₂ = 0.0928

$$R_1 = \frac{\sum \|F_o\| - |F_c|}{\sum |F_o|}; wR_2 = [\frac{\sum w(F_o^2 - F_c^2)^2}{\sum w(F_o^2)^2}]^{1/2}.$$

2.4. Antifungal Activity

In this research, seven plant fungi, including *Rhizoctonia solani* AG1, *Phytophthora parasitica* var. *nicotianae*, *Fusarium verticillioides*, *Sphaeropsis sapinea*, *Fusarium oxysporum* f. sp. *Niveum*, *Colletotrichum fructicola*, and *Colletotrichum acutatum* were used for assessing the antifungal activity of these compounds using mycelial growth rate method. The compounds in a mixture of DMSO and Tween 80 (less than 0.5%) were further diluted to 150 mg/L and 300 mg/L in a PDA plate to obtain a stock solution (1.0 × 10⁴ mg/L). After PDA solidified, a 5 mm diameter fungus cake was acquired from the edge of the pathogenic fungi colony cultured for 7 days with an inoculation ring. The fungus cake was moved to the center of the Petri dishes, with the hyphae facing down. After the treatment, the Petri dishes were placed in a constant temperature biochemical incubator at 28 °C for cultivation, and the growth diameter of the hyphae was measured after 3–10 days. As a positive control, azoxystrobin and tricyclazole (antifungal agent) were used. The solution without the test compound was used as a blank control. All experiments were repeated three times independently. Finally, the inhibition rate (%) of mycelium growth was calculated using SPSS statistical software.

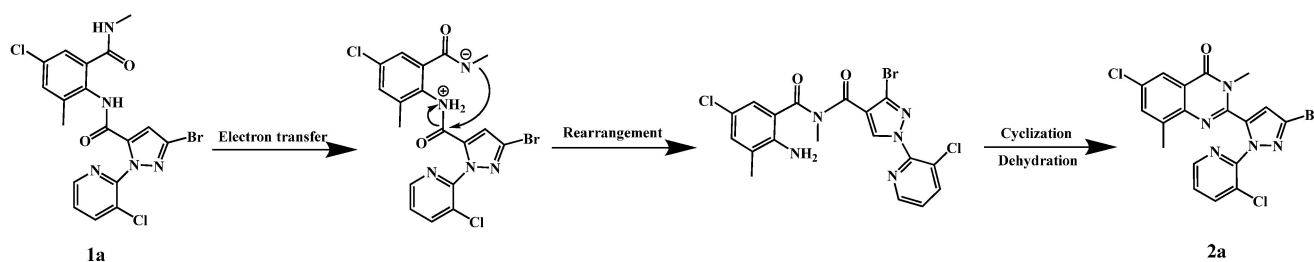
Table 2. Selected bond lengths (Å) and bond angles (°) of **2a**.

Bond	Bond Lengths/(Å)	Angle	Bond Angle/(°)	Angle	Bond Angle/(°)
C(1)-C(2)	1.498(4)	C(3)-C(2)-C(7)	118.0(3)	C(16)-C(15)-C(14)	118.4(2)
C(2)-C(3)	1.381(4)	C(3)-C(2)-C(1)	121.3(3)	C(16)-C(15)-Cl(2)	120.1(2)
C(2)-C(7)	1.409(4)	C(7)-C(2)-C(1)	120.6(2)	C(14)-C(15)-Cl(2)	121.41(19)
C(3)-C(4)	1.389(4)	C(2)-C(3)-C(4)	121.1(3)	C(17)-C(16)-C(15)	118.6(3)
C(4)-C(5)	1.376(4)	C(5)-C(4)-C(3)	121.5(2)	C(16)-C(17)-C(18)	118.9(3)
C(4)-Cl(1)	1.735(3)	C(5)-C(4)-Cl(1)	119.1(2)	N(5)-C(18)-C(17)	123.2(3)
C(5)-C(6)	1.389(4)	C(3)-C(4)-Cl(1)	119.3(2)	C(10)-N(1)-C(7)	118.6(2)
C(6)-C(7)	1.400(4)	C(4)-C(5)-C(6)	118.2(3)	C(10)-N(2)-C(8)	120.9(2)
C(6)-C(8)	1.464(4)	C(5)-C(6)-C(7)	121.0(3)	C(10)-N(2)-C(9)	121.8(2)
C(7)-N(1)	1.382(3)	C(5)-C(6)-C(8)	119.6(2)	C(8)-N(2)-C(9)	117.1(2)
C(8)-O(1)	1.219(3)	C(7)-C(6)-C(8)	119.4(2)	N(4)-N(3)-C(11)	112.34(18)
C(8)-N(2)	1.393(3)	N(1)-C(7)-C(6)	121.2(2)	N(4)-N(3)-C(14)	119.39(19)
C(9)-N(2)	1.474(3)	N(1)-C(7)-C(2)	118.7(2)	C(11)-N(3)-C(14)	127.90(19)
C(10)-N(1)	1.290(3)	C(6)-C(7)-C(2)	120.1(2)	C(13)-N(4)-N(3)	103.23(19)
C(10)-N(2)	1.385(3)	O(1)-C(8)-N(2)	120.8(2)	C(14)-N(5)-C(18)	117.4(2)
C(10)-C(11)	1.470(3)	O(1)-C(8)-C(6)	124.2(2)		
C(11)-N(3)	1.363(3)	N(2)-C(8)-C(6)	115.0(2)		
C(11)-C(12)	1.372(3)	N(1)-C(10)-N(2)	124.7(2)		
C(12)-C(13)	1.388(4)	N(1)-C(10)-C(11)	116.6(2)		
C(13)-N(4)	1.318(3)	N(2)-C(10)-C(11)	118.7(2)		
C(13)-Br(1)	1.866(2)	N(3)-C(11)-C(12)	106.3(2)		
C(14)-N(5)	1.321(3)	N(3)-C(11)-C(10)	119.9(2)		
C(14)-C(15)	1.384(3)	C(12)-C(11)-C(10)	133.2(2)		
C(14)-N(3)	1.425(3)	C(11)-C(12)-C(13)	104.4(2)		
C(15)-C(16)	1.378(4)	N(4)-C(13)-C(12)	113.7(2)		
C(15)-Cl(2)	1.717(3)	N(4)-C(13)-Br(1)	120.15(18)		
C(16)-C(17)	1.375(4)	C(12)-C(13)-Br(1)	126.11(19)		
C(17)-C(18)	1.376(5)	N(5)-C(14)-C(15)	123.5(2)		
C(18)-N(5)	1.333(4)	N(5)-C(14)-N(3)	115.8(2)		
N(3)-N(4)	1.360(3)	C(15)-C(14)-N(3)	120.7(2)		

3. Results and Discussion

3.1. Chemistry

The reaction was carried out in a one-pot method at constant temperature using four compounds (**1a**~**1d**) containing bisamide structures as starting materials. The reaction uses aqueous methylamine solution as a catalyst, and the reactants undergo Smiles rearrangement [18] under alkaline conditions, then undergo intramolecular cyclization and dehydration to obtain the product. According to the conversion process of the reaction, considering reactant **1a** as an example, the reaction mechanism is deduced, as shown in Scheme 2. The synthetic route has the advantages of mild reaction process, fast reaction progress, simple reaction operation, few by-products, and so on.

**Scheme 2.** Prediction of the reaction mechanism for the synthesis of product **2a**.

During the experiment, considering the synthesis of target compound **2a** as an example, the reaction conditions suitable for the reaction were determined by changing the conditions, i.e., catalyst, solvent, and reaction temperature, and monitoring the yield of

compound **2a** under different reaction conditions (Table 3). Methylamine hydrochloride, triethylamine, pyridine, sodium carbonate, and methylamine aqueous solution were used as catalysts to participate in the reaction. After 4 h of reaction in the system with the same reaction conditions, it was found that methylamine hydrochloride and pyridine could not be used as catalysts in this experiment. When triethylamine, sodium carbonate, and methylamine aqueous solutions were used as catalysts, the reactions all proceeded normally, but the yields of compound **2a** varied, with methylamine aqueous solution being the best. Under the catalysis of methylamine aqueous solution, the yield of compound **2a** reached the maximum at 4 h and remained almost unchanged by shortening or prolonging the reaction time. We also selected several solvents with different boiling points and soluble with water to participate in the reaction, trying to improve the reaction efficiency by changing the solvent. The results showed that the yield of compound **2a** increased with the increase of solvent boiling point for the five solvents in reflux state. For the high-boiling solvent DMF, an increase in the reaction temperature from 90 °C to 100 °C also exhibited a small increase in yield. However, when 1,4-dioxane was used as solvent, the reaction efficiency basically reaches the highest at 90 °C, and the yield of compound **2a** does not increase with the increase of temperature. In summary, the reaction of the initial compound at 90 °C for 4 h in the system with aqueous methylamine as catalyst and 1, 4-dioxane as solvent resulted in the highest yield of the target compound.

Table 3. Reaction yield under different conditions.

Catalyst	Solvent	Temperature	Time (h)	Yield (%)
CH ₃ -NH ₂ · HCl	1,4-Dioxane	90 °C	4	-
(CH ₃ CH ₂) ₃ N	1,4-Dioxane	90 °C	4	74.63
Pyridine	1,4-Dioxane	90 °C	4	-
Na ₂ CO ₃	1,4-Dioxane	90 °C	4	69.75
CH ₃ -NH ₂ · H ₂ O	1,4-Dioxane	90 °C	4	87.33
CH ₃ -NH ₂ · H ₂ O	1,4-Dioxane	90 °C	2	57.82
CH ₃ -NH ₂ · H ₂ O	1,4-Dioxane	90 °C	3	77.06
CH ₃ -NH ₂ · H ₂ O	1,4-Dioxane	90 °C	5	86.89
CH ₃ -NH ₂ · H ₂ O	Acetone	Reflux	4	37.56
CH ₃ -NH ₂ · H ₂ O	MeOH	Reflux	4	44.90
CH ₃ -NH ₂ · H ₂ O	THF	Reflux	4	55.38
CH ₃ -NH ₂ · H ₂ O	MeCN	Reflux	4	69.72
CH ₃ -NH ₂ · H ₂ O	DMF	90 °C	4	20.67
CH ₃ -NH ₂ · H ₂ O	DMF	100 °C	4	32.48
CH ₃ -NH ₂ · H ₂ O	1,4-Dioxane	80 °C	4	79.49
CH ₃ -NH ₂ · H ₂ O	1,4-Dioxane	Reflux	4	87.28

The “-” means that the reaction does not occur.

The structures of the four products were confirmed to be correct using characterization methods, such as FT-IR, ¹H NMR, ¹³CNMR, and HRMS, and the crystal structure of **2a** was analyzed using X-ray diffraction to further confirm the product structure.

3.2. Structural Characterization Analysis

All compounds were characterized using infrared spectroscopy in the range of 400–4000 cm⁻¹. In compounds **2a**–**2d**, the peak appearing at about 3100 cm⁻¹ is indicative of C-H stretching vibration of unsaturated carbons. The stretching vibration peak around 3000 cm⁻¹ is due to C-H on the benzene ring. The absorption peak of C-H on the methyl group appeared at 2950 cm⁻¹. A particularly obvious absorption peak appeared around 1680 cm⁻¹, which belonged to C=O. In addition, the aromatic ring can be further confirmed by the continuous peak packets appearing in the shape of fingers at 1400–1600 cm⁻¹. The absorption peak of several halogens in the compounds are in the range of 500–800 cm⁻¹. In addition, the cyano group in **2c** and **2d** showed a distinct absorption peak at 2230 cm⁻¹ (In Supplementary Materials).

In the ^1H NMR spectra of the compounds, the protons whose chemical shifts appeared in the 8.42–7.31 ppm region belonged to aromatic rings (phenyl and pyridine rings), which have been basically consistent with those presented by the simulated spectra. The chemical shift of the proton on the pyrazole ring appears around 6.87 ppm and exists in the form of a single peak. The methyl group attached to the nitrogen on the quinazolinone structure is presented as a single peak at 6.87 ppm. The proton attached to the methyl group of the phenyl ring appears as a singlet at 2.03 ppm. Generally speaking, the multiple peak morphologies of these four compounds along with the number of protons are consistent with the simulated spectra to a great extent.

In the ^{13}C NMR spectra of the compounds, all carbons of the aromatic ring clearly appear in the range of 109~161 ppm, and the carbon of the carbonyl group, having the highest chemical shift, appears near 161 ppm. The methyl groups on the quinazolinones appear at 16 ppm and 33 ppm. From the above characterization data, the correctness of the structure of the compound can be basically established.

3.3. Crystal Structure of 2a

Compound **2a** crystallizes in the monoclinic space group P 21/c. In the molecule of **2a** (Figure 1), bond lengths and angles are very similar to those given in the literature for chalcone derivatives [19]. The part of quinazoline was approximately planar. The dihedral angles of the C2–C7 phenyl plane, the pyrazole ring, and the pyridine ring plane were $39.728(85)^\circ$, $63.024(90)^\circ$ and $56.700(76)^\circ$, respectively. Compound **2a** forms a three-dimensional structure by π – π stacking (Figure 2).

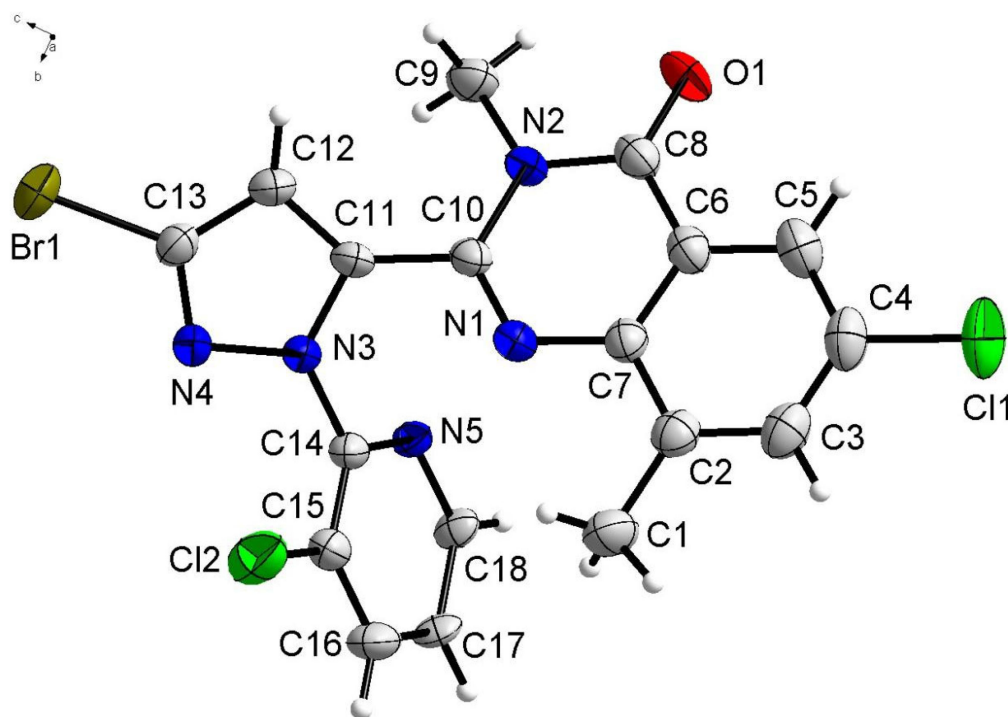


Figure 1. Crystal structure of **2a** with 30% thermal ellipsoids.

3.4. Structure-Activity Relationship (SAR)

Compounds **2a**–**2d** have been tested in laboratory to inhibit seven kinds of plant pathogenic fungi (*Rhizoctonia solani* AG1, *Phytophthora parasitica* var. *nicotianae*, *Fusarium verticillioides*, *Sphaeropsis sapinea*, *Fusarium oxysporum* f. sp. *Niveum*, *Colletotrichum fructicola*, and *Colletotrichum acutatum*) at concentrations of 150 and 300 mg/L, respectively. The mycelial growth rate method was applied, by measuring the colony diameter, and the inhibition rate was calculated (Table 4). The broad-spectrum fungicide tricyclazole was

used as a positive control, and the test results showed that all compounds had some antifungal activity.

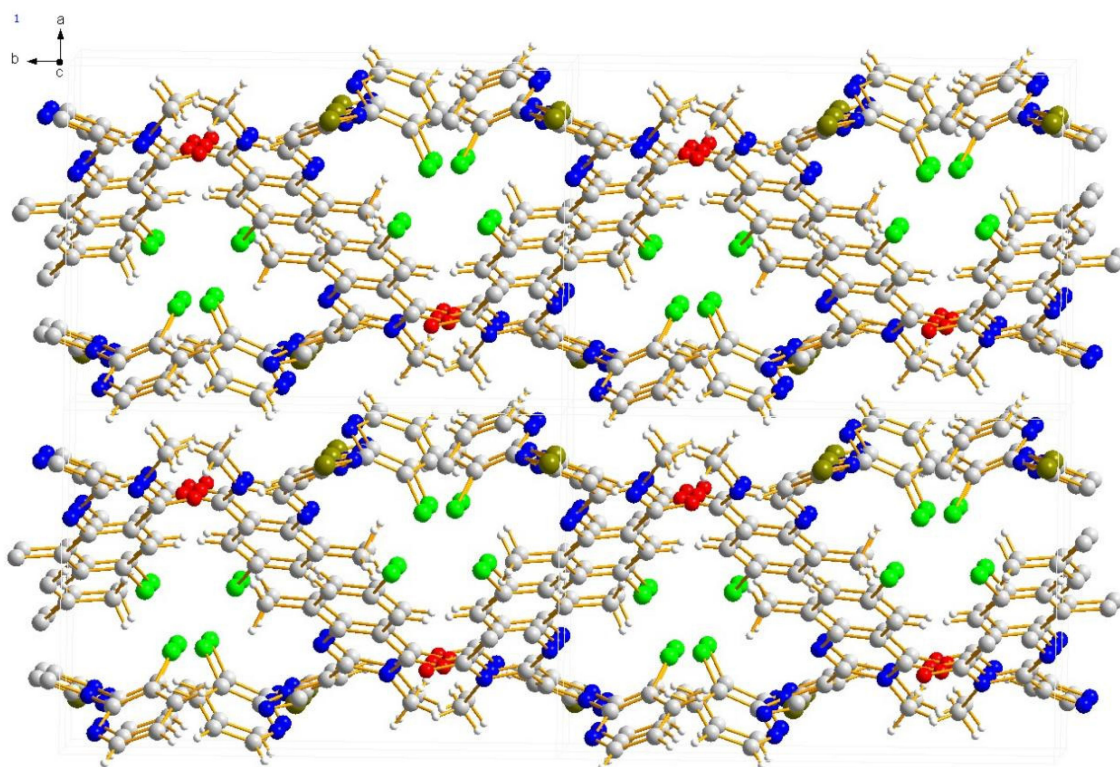


Figure 2. Stacking structure of compound 2a.

Table 4. Antifungal activity of compounds 2a~2d.

Compd	Conc (mg/L)	Inhibition Rate (%) \pm SD						
		R. S.	P. P.	F. V.	S. S.	F. N.	C. F.	C. A.
2a	150	25.11 \pm 0.12	22.53 \pm 0.46	7.91 \pm 1.20	18.89 \pm 0.65	21.66 \pm 0.98	17.22 \pm 1.08	16.23 \pm 1.73
	300	55.00 \pm 2.12	46.42 \pm 1.77	21.59 \pm 1.56	41.82 \pm 0.90	38.90 \pm 1.64	26.22 \pm 2.07	35.32 \pm 1.45
2b	150	29.73 \pm 0.20	13.73 \pm 0.65	9.44 \pm 0.40	11.20 \pm 1.48	11.58 \pm 0.36	11.00 \pm 1.47	11.30 \pm 0.37
	300	59.60 \pm 1.00	27.55 \pm 0.87	18.72 \pm 0.76	20.00 \pm 0.93	25.96 \pm 0.75	21.02 \pm 1.21	26.88 \pm 0.65
2c	150	10.74 \pm 1.35	18.66 \pm 0.76	18.62 \pm 1.04	7.52 \pm 0.91	35.37 \pm 1.55	31.92 \pm 1.05	14.29 \pm 1.47
	300	29.25 \pm 0.55	37.50 \pm 0.60	41.82 \pm 1.20	16.22 \pm 1.49	62.42 \pm 1.46	54.60 \pm 0.30	34.68 \pm 1.36
2d	150	11.72 \pm 2.02	18.68 \pm 1.47	21.23 \pm 0.88	8.66 \pm 2.10	32.24 \pm 0.86	36.02 \pm 1.08	7.24 \pm 2.05
	300	30.6 \pm 1.99	39.02 \pm 1.35	40.60 \pm 2.20	17.28 \pm 1.00	57.88 \pm 1.24	55.41 \pm 1.52	20.39 \pm 0.56
TCZ	150	74.24 \pm 2.50	44.72 \pm 0.56	40.20 \pm 2.41	40.02 \pm 0.38	55.80 \pm 1.10	78.43 \pm 2.00	65.70 \pm 0.58
	300	97.00 \pm 1.56	83.02 \pm 0.76	67.58 \pm 1.30	66.28 \pm 1.02	79.03 \pm 1.35	98.01 \pm 0.47	80.20 \pm 1.00

Data are given as the mean of triplicate experiments. R. S., *Rhizoctonia solani* AG1; P. P., *Phytophthora parasitica* var. *nicotianae*; F. V., *Fusarium verticillioides*. S. S., *Sphaeropsis sapinea*; F. N., *Fusarium oxysporum* f. sp. *Niveum*; C. F., *Colletotrichum fructicola*. C. A., *Colletotrichum acutatum*. TCZ, *tricyclazole*.

Importantly, the results show that for fungus *Rhizoctonia solani* AG1, the inhibition effect is better when the connecting group on the quinazolinone group is chloride (compounds 2a and 2b) than when the connecting group on the quinazolinone group is cyano group (compounds 2c and 2d). The higher the chlorine content, the better is the antifungal effect. Against fungi *Fusarium verticillioides*, *Fusarium oxysporum* f. sp. *Niveum*, and *Colletotrichum fructicola*, compounds 2c and 2d containing cyano group have better inhibitory effect than compounds 2a and 2b. At concentrations of 150 and 300 mg/L, compound 2b had the best inhibitory activity against *Phytophthora parasitica* var. *nicotianae*.

4. Conclusions

In this paper, four kinds of quinazolinones were synthesized from four diamide-containing compounds catalyzed by methylamine aqueous solution. Their chemical structures were characterized using ^1H NMR, ^{13}C NMR, FT-IR, and HRMS. In the antifungal bioassay, it was found that these four new compounds had certain inhibitory effects on the growth of seven plant pathogenic fungi. The results showed that the existence of chlorine in compounds **2a** and **2b** had an obvious inhibitory effect on *Rhizoctonia solani* AG1. Although the antifungal activity of most compounds is weaker than that of the positive control, to the best of my knowledge, there are very few antifungal agents with this structure. It is necessary to optimize their structure to further develop better antifungal agents against plant pathogenic fungi.

Supplementary Materials: The following supporting information can be downloaded at: <https://www.mdpi.com/article/10.3390/cryst13081254/s1>, Figure S1: The ^1H NMR spectra Compound **2a**; Figure S2: The ^{13}C NMR spectra Compound **2a**; Figure S3: The FT-IR spectra of Compound **2a**; Figure S4: The HRMS spectra of Compound **2a**; Figure S5: The ^1H NMR spectra Compound **2b**; Figure S6: The ^{13}C NMR spectra Compound **2b**; Figure S7: The FT-IR spectra of Compound **2b**; Figure S8: The HRMS spectra of Compound **2b**; Figure S9: The ^1H NMR spectra Compound **2c**; Figure S10: The ^{13}C NMR spectra Compound **2c**; Figure S11: The FT-IR spectra of Compound **2c**; Figure S12: The HRMS spectra of Compound **2c**; Figure S13: The ^1H NMR spectra Compound **2d**; Figure S14: The ^{13}C NMR spectra Compound **2d**; Figure S15: The FT-IR spectra of Compound **2d**; Figure S16: The HRMS spectra of Compound **2d**; Supplementary Files: SF1: CIF for **2a**; SF2: CheckCIF report for **2a**.

Author Contributions: R.Z.: methodology, validation, investigation, data curation, writing—original draft. C.H.: data analysis. J.W.: investigation. Y.Z.: methodology. Q.F.: data analysis. S.X.: data curation. X.N.: conceptualization, methodology. S.C.: review and editing, supervision, project administration, funding acquisition. D.P.: review and editing, conceptualization, supervision, project administration, funding acquisition. All authors have read and agreed to the published version of the manuscript.

Funding: This research was funded by the National Natural Science Foundation (No. 31960295, No. 32160660, No. 21562022), Jiangxi Province Academic and Technical Leaders Training Program Leading Talents Project (20204BCJ22022), Special Funding for Major Scientific and Technological Research and Development in Jiangxi Province (20203ABC28W016), Special Research Project on CamphorTree (KRPCT) of Jiangxi Forestry Department (grant No. 2020CXZX07), the Research Foundation of Jiangxi Provincial Drug Administration [2021-03,2022-03], and the Earmarked Fund for the Youthful Innovation Research Team of Jiangxi Agricultural University-05, 2021 Innovation Team project of Ji'an City, Jiangxi Province.

Informed Consent Statement: Not applicable.

Data Availability Statement: Data are contained within the manuscript.

Conflicts of Interest: The authors declare that there are no conflicts of interest.

References

1. Chatterjee, S.; Kuang, Y.; Splivallo, R.; Chatterjee, P.; Karlovsky, P. Interactions among filamentous fungi *Aspergillus niger*, *Fusarium verticillioides* and *Clonostachys rosea*: Fungal biomass, diversity of secreted metabolites and fumonisin production. *BMC Microbiol.* **2016**, *16*, 83. [CrossRef]
2. Peng, Y.; Li, S.J.; Yan, J.; Tang, Y.; Cheng, J.P.; Gao, A.J.; Yao, X.; Ruan, J.J.; Xu, B.L. Research Progress on Phytopathogenic Fungi and Their Role as Biocontrol Agents. *Front. Microbiol.* **2021**, *12*, 670135. [CrossRef] [PubMed]
3. Marín-Menguiano, M.; Moreno-Sánchez, I.; Barrales, R.R.; Fernández-Álvarez, A.; Ibeas, J.I. N-glycosylation of the protein disulfide isomerase Pdi1 ensures full *Ustilago maydis* virulence. *PLoS Pathog.* **2019**, *15*, e1007687. [CrossRef] [PubMed]
4. Kerru, N.; Gummidi, L.; Maddila, S.; Gangu, K.K.; Jonnalagadda, S.B. A Review on Recent Advances in Nitrogen-Containing Molecules and Their Biological Applications. *Molecules* **2020**, *25*, 1909. [CrossRef] [PubMed]
5. Naito, T. Development of new synthetic reactions for nitrogen-containing compounds and their application. *Chem. Pharm. Bull.* **2008**, *56*, 1367–1383. [CrossRef] [PubMed]

6. Xiang, W.; Chenghao, T.; Xianghui, J.; Shaoyun, W.; Guohui, Z.; Tizhong, G.; Xiuhong, H. Recent advances on the synthesis and pesticidal activity evaluations of quinazoline derivatives. *Chin. J. Pestic. Sci./Nongyaoxue Xuebao* **2017**, *19*, 131–151.
7. Gupta, T.; Rohilla, A.; Pathak, A.; Akhtar, M.J.; Haider, M.R.; Yar, M.S. Current perspectives on quinazolines with potent biological activities: A review. *Synth. Commun.* **2018**, *48*, 1099–1127. [[CrossRef](#)]
8. Chen, J.; Wang, Y.; Luo, X.; Chen, Y. Recent research progress and outlook in agricultural chemical discovery based on quinazoline scaffold. *Pestic. Biochem. Physiol.* **2022**, *184*, 105122. [[CrossRef](#)] [[PubMed](#)]
9. Antipenko, L.; Karpenko, A.; Kovalenko, S.; Katsev, A.; Komarovska-Porokhnyavets, E.; Novikov, V.; Chekotilo, A. Synthesis of new 2-thio-[1, 2, 4] triazolo [1, 5-c] quinazoline derivatives and its antimicrobial activity. *Chem. Pharm. Bull.* **2009**, *57*, 580–585. [[CrossRef](#)] [[PubMed](#)]
10. Latli, B.; Wood, E.; Casida, J.E. Insecticidal Quinazoline Derivatives with (Trifluoromethyl)diaziriny and Azido Substituents as NADH: Ubiquinone Oxidoreductase Inhibitors and Candidate Photoaffinity Probes. *Chem. Res. Toxicol.* **1996**, *9*, 445–450. [[CrossRef](#)] [[PubMed](#)]
11. Paneersalvam, P.; Raj, T.; Ishar, M.; Singh, B.; Sharma, V.; Rather, B. Anticonvulsant activity of schiff bases of 3-amino-6,8-dibromo-2-phenyl-quinazolin-4(3H)-ones. *Indian J. Pharm. Sci.* **2010**, *72*, 375–378. [[CrossRef](#)] [[PubMed](#)]
12. Nandy, P.; Vishalakshi, M.; Bhat, A. Synthesis and antitubercular activity of Mannich bases of 2-methyl-3H-quinazolin-4-ones. *Indian J. Heterocycl. Chem.* **2006**, *15*, 293–294.
13. Saravanan, G.; Alagarsamy, V.; Prakash, C.R. Synthesis and evaluation of antioxidant activities of novel quinazoline derivatives. *Int. J. Pharm. Pharm. Sci.* **2010**, *2*, 83–86.
14. Hess, H.J.; Cronin, T.H.; Scriabine, A. Antihypertensive 2-amino-4(3H)-quinazolinones. *J. Med. Chem.* **1968**, *11*, 130–136. [[CrossRef](#)] [[PubMed](#)]
15. Lakhan, R.; Singh, O.P.; Singh, J.R.L. Studies on 4 (3H)-quinazolinone derivatives as anti-malarials. *Indian Chem. Soc.* **1987**, *64*, 316–318.
16. Kumar, K.A.; Jayaroopa, P. Pyrazoles: Synthetic strategies and their pharmaceutical applications-an overview. *Int. J. PharmTech Res.* **2013**, *5*, 1473–1486.
17. Habib, O.M.; Hassan, H.M.; El-Mekabaty, A. Novel quinazolinone derivatives: Synthesis and antimicrobial activity. *Med. Chem. Res.* **2012**, *22*, 507–519. [[CrossRef](#)]
18. Bunnett, J.F.; Zahler, R.E. Aromatic Nucleophilic Substitution Reactions. *Chem. Rev.* **1951**, *49*, 273–412. [[CrossRef](#)]
19. Torralba, M.; Cano, M.; Campo, J.; Heras, J.; Pinilla, E. Crystal structure of 2-[3, 5-bis (4-octyloxyphenyl) pyrazol-1-yl] pyridine, C₃₆H₄₇N₃O₂. *Z. Für Krist.-New Cryst. Struct.* **2005**, *220*, 647–649. [[CrossRef](#)]

Disclaimer/Publisher's Note: The statements, opinions and data contained in all publications are solely those of the individual author(s) and contributor(s) and not of MDPI and/or the editor(s). MDPI and/or the editor(s) disclaim responsibility for any injury to people or property resulting from any ideas, methods, instructions or products referred to in the content.